

[1]

A physically based, two-dimensional, finite-difference algorithm for modeling variably saturated flow

T.P. Clement¹, William R. Wise*, Fred J. Molz

Department of Civil Engineering, 238 Harbert Engineering Center, Auburn University, Auburn, AL 36849-5337, USA

Received 30 July 1993; revision accepted 16 March 1994

Abstract

A computationally simple, numerical algorithm capable of solving a wide variety of two-dimensional, variably saturated flow problems is developed. Recent advances in modeling variably saturated flow are incorporated into the algorithm. A physically based form of the general, variably saturated flow equation is solved using finite differences (centered in space, fully implicit in time) employing the modified Picard iteration scheme to determine the temporal derivative of the water content. The algorithm avoids mass-balance errors in unsaturated regions and is numerically stable. The resulting system of linear equations is solved by a preconditioned conjugate gradient method, which is known to be computationally efficient for the type of equation set obtained. The algorithm is presented in sufficient detail to allow others to implement it easily, and is verified using four published, illustrative sets of experimental data.

1. Introduction

Many water-related problems of current interest involve variably saturated porous media. Such problems include wetland and beach environments, ground excavations, earthen dams, and groundwater pumping systems in unconfined aquifers. Models are needed to study the response in such systems as a result of environmental controls, both naturally and anthropogenically imposed. In particular, finite-difference algorithms offer three major advantages: ease of coding, ease of data input, and more ready public acceptance (in comparison with finite-element models). In the

* Corresponding author.

¹ Present address: Battelle, Pacific Northwest Laboratories, Battelle Boulevard, P.O. Box 999, Richland, WA 99352, USA.

present work, recent advances in modeling variably saturated flow are incorporated into a comprehensive, finite-difference variably saturated flow model.

Several numerical models have been developed for simulating the movement of water in variably saturated porous media. Many of these are listed in Table 1. In most applications, the pressure-based form of the variably saturated flow equation is used (Neuman, 1973; Cooley, 1983; Huyakorn et al., 1984, 1986). Unfortunately, numerical solutions of the pressure-based form of the closely related, but more restrictive, Richards' equation are known to have poor mass-balance properties in unsaturated media (Celia et al., 1990; Kirkland, 1991). In the literature, a variety of numerical schemes including finite-difference, integrated finite difference, and finite-element methods have been used to solve variably saturated flow problems (Neuman, 1973; Narasimhan and Witherspoon, 1976; Cooley, 1983; Huyakorn et al., 1984, 1986).

Finite-difference approximations have been widely used in several studies solving one-dimensional (vertical), variably saturated flow problems (e.g. Day and Luthin, 1956; Whisler and Watson, 1968; Freeze, 1969; Brandt et al., 1971; Haverkamp et al., 1977; Dane and Mathis, 1981; Haverkamp and Vauclin, 1981). Fewer researchers have used finite differences to solve variably saturated flow problems in higher dimensions (e.g. Rubin, 1968; Cooley, 1971; Freeze, 1971a,b; Kirkland et al., 1992). Most of the existing two-dimensional finite-difference solutions to variably saturated flow problems have limitations. The finite-difference models of Freeze (1971a,b) and Cooley (1971) are not robust because they incur numerical instabilities and convergence difficulties. These problems arise primarily from inefficiencies of the line successive over-relaxation and alternating directional implicit schemes used in solving the two-dimensional, nonlinear equations. In the authors' opinion, Kirkland et al. (1992) presented the most successful and efficient example of a finite-difference solution to two-dimensional, variably saturated flow problems. However, the objective of Kirkland et al. (1992) was to develop competitive numerical procedures to solve infiltration problems in dry soils. The fundamental flow equation solved by Kirkland et al. (1992) (Richards' equation) does not account for the effects of specific storage, and consequently it cannot be used to model accurately a wide variety of variably saturated flow problems, including many transient drainage and seepage-face phenomena in large domains.

Finite elements have been successfully used by several researchers to solve the general variably saturated flow equation (e.g. Neuman, 1973; Cooley, 1983; Huyakorn et al., 1984; Huyakorn et al., 1986). However, all of these finite-element models use pressure-based, finite-difference, Euler time marching algorithms to approximate the transient term, which can produce high mass-balance errors. Panday et al. (1993) discussed recent advances in finite-element modeling techniques for variably saturated flow problems.

The objective of the present work is to develop and present a computationally simple and efficient finite-difference algorithm that can solve a wide variety of two-dimensional, variably saturated flow problems. A mixed form of the general variably saturated flow equation is solved using finite differences employing the modified Picard iteration scheme presented by Celia et al. (1990), who used it to solve the mixed form of Richards' equation in one dimension. The resulting system of linear

Table 1
Summary of saturated–unsaturated flow models

Model	Equations	Solution procedure
Rubin (1968)	Pressure-based 2-D Richards' equation	Finite-difference; alternating direction implicit (ADI) or an iterative ADI
Freeze (1971a,b)	Pressure-based 3-D general variably saturated flow	Finite-difference; line successive over-relaxation
Brutsaert (1971)	Mixed form of 2-D Richards' equation	Finite-difference; Newton–Raphson iteration; Gauss elimination
UNSAT2 Neuman (1973)	Pressure-based 2-D general variably saturated flow	Finite-element; Gauss elimination
TRUST Narasimhan et al. (1978)	Pressure-based for variably saturated flow and water content based unsaturated flow problems	Integrated finite difference; mixed explicit–implicit time-stepping procedure
FEMWATER Yeh and Ward (1981)	Pressure-based 2-D general variably saturated flow	Finite-element; with Gauss elimination (or point iteration)
3-D FEMWATER Yeh (1992)	Pressure-based 3-D Richard's equation	Finite-element; Gauss elimination; successive block or point iteration
Cooley (1983)	Pressure-based 2-D general variably saturated flow	Sub-domain finite-element; combination of Newton–Raphson and strongly implicit procedure
SATURN Huyakorn et al. (1984)	Pressure-based 2-D general variably saturated flow	Finite-element (influence coefficient); Newton–Raphson or Picard iteration; LU decomposition
FLAMINCO Huyakorn et al. (1986)	Pressure-based 3-D general variably saturated flow	Finite-element (influence coefficient); Picard iteration; slice successive over-relaxation LU decomposition
Allen and Murphy (1986)	Mixed form of Richards' equation	Collocation finite-element; Gauss elimination
VS2DT Healy (1990)	Pressure-based form of general variably saturated flow	Finite-difference; strongly implicit procedure
Kirkland et al. (1992)	Transformed, pressure-based and mixed forms of 2-D Richards' equation	Finite-difference; preconditioned conjugate gradient method

equations is solved by a preconditioned conjugate gradient method. One purpose of this paper is to collect many of the recent developments in this area into one tractable discussion, and thus serve in a tutorial role.

Solving variably saturated flow problems using the above procedure has the following advantages:

(1) the mixed form of the variably saturated flow equation can be solved in a computationally efficient manner and is capable of modeling a wide variety of problems, including infiltration into dry soils (see, e.g. Kirkland et al., 1992).

(2) The modified Picard iterative procedure for the mixed form of the variably saturated flow equation is fully mass conserving in the unsaturated zone. By contrast, conventional, pressure-based, backward Euler finite-difference formulations exhibit poor mass-balance behavior arising from the manner in which the time derivative, $\partial\theta/\partial t$, is approximated as $C(\Psi)\partial\Psi/\partial t$, where $C(\Psi) = d\theta/d\Psi$ is the specific moisture capacity. Even though this approximation is valid mathematically in a continuous partial differential equation, the discrete analogs of $\partial\theta/\partial t$ and $C(\Psi)\partial\Psi/\partial t$ are not equivalent. This inequality is amplified owing to the highly non-linear nature of the specific capacity term, $C(\Psi)$. Using the modified Picard approach eliminates this problem by directly approximating the temporal term $\partial\theta/\partial t$ with its algebraic analog. A detailed analysis of the mass conservative properties of the modified Picard solution to the mixed form of Richards' equation has been given by Celia et al. (1990). The mass conservation property, which applies in the unsaturated zone, is not restricted to Richards' equation; it also applies to the general variably saturated flow equation, which accounts for the compressibility effects which Richards' equation neglects.

(3) Spatial approximation of the variably saturated flow equation using the finite-difference method is naturally mass lumping, in contrast to common formulations of the finite-element method, which require mass lumping to avoid oscillatory solutions (Celia et al., 1990).

(4) The preconditioned conjugate gradient method used for solving the set of finite-difference equations is computationally efficient, highly stable, and requires minimum computer storage and time.

In the following section, a finite-difference algorithm for solving the mixed form of the variably saturated flow equation is presented in sufficient detail to allow others to implement it easily to solve a broad variety of variably saturated flow problems. The contributions of this algorithm include the extension of the mass-conservative form of the solution method to two dimensions and accounting for the effects of specific storage, which can be significant for many transient drainage problems.

2. Theory

The governing equation for variably saturated flow through homogeneous and isotropic porous media is conventionally written in pressure-based form as

$$S_s \frac{\theta}{\eta} \frac{\partial\Psi}{\partial t} + \frac{d\theta}{d\Psi} \frac{\partial\Psi}{\partial t} = \nabla \cdot K(\Psi) \{ \nabla\Psi + \hat{k} \} \quad (1)$$

where S_s is the specific storage of the medium (L^{-1}), Ψ is the pressure head (L), θ is the water content, η is the porosity, $K(\Psi)$ is the hydraulic conductivity ($L T^{-1}$), t is time [T], and \hat{k} is the unit-upward vector (Pinder and Gray, 1977). Eq. (1) describes the movement of water in an isotropic soil matrix, and is derived based on the following assumptions: (1) the dynamics of the air phase do not affect those of the water phase; (2) the density of water is only a function of pressure; (3) the spatial gradient of the water density is negligible (Pinder and Gray, 1977). In the unsaturated region, Eq. (1) effectively reduces to Richards' equation, as the second term on the left side tends to dominate the first term on that side.

2.1. Most direct mathematical description of the physics involved with variably saturated flow

It should be noted that both terms on the left side of Eq. (1) are expressed in terms of the time derivative of the pressure head, Ψ , rather than the moisture content, θ . For the first term, $(S_s\theta/\eta)\partial\Psi/\partial t$, this is physically representative of the fact that the effects of specific storage are due to changes in pressure. This storage variation is due to the temporal changes in fluid density and formation porosity. The second term in Eq. (1) describes the effects of draining and filling pores, so statement in terms of the temporal change in moisture content is more appropriate than description via the pressure. In other words, the term $(d\theta/d\Psi)\partial\Psi/\partial t$ is more appropriately written in its simpler form: $\partial\theta/\partial t$. On the right side of Eq. (1), it should be noted that the spatial derivative of the hydraulic head is used to describe the driving force for fluid movement. This is the most direct mathematical statement of the fact that head differences do indeed supply the energy required to move fluid. Specification of the hydraulic conductivity as a function of the pressure head, $K(\Psi)$, is, however, not directly representative of the underlying physics. It is water-filled pores which facilitate transmission of water through a porous medium. The fact that, in modeling water behavior in the unsaturated zone, water content and pressure are directly related (through the capillary pressure function) is secondary to the underlying physics of the flow. Consequently, the hydraulic conductivity, formally, should be expressed in terms of the moisture content, $K(\theta)$. (This has hidden advantages for modeling purposes, such as the fact that $K(\Psi)$ typically exhibits hysteresis, whereas $K(\theta)$ exhibits relatively little (Dullien, 1979, p. 258).) Hence, the most direct mathematical expression of the physics of variably saturated flow, given the considerations discussed above, is

$$S_s \frac{\theta}{\eta} \frac{\partial\Psi}{\partial t} + \frac{\partial\theta}{\partial t} = \nabla \cdot K(\theta) \{ \nabla\Psi + \hat{k} \} \quad (2)$$

This form of the variably saturated flow equation usually appears, if at all, only during derivation of the pressure-based form, Eq. (1). For two-dimensional flow, the general flow equation, Eq. (2), written in expanded notation, is

$$S_s \frac{\theta}{\eta} \frac{\partial\Psi}{\partial t} + \frac{\partial\theta}{\partial t} = \frac{\partial}{\partial x} \left\{ K(\theta) \frac{\partial\Psi}{\partial x} \right\} + \frac{\partial}{\partial z} \left\{ K(\theta) \frac{\partial\Psi}{\partial z} \right\} + \frac{\partial K(\theta)}{\partial z} \quad (3)$$

where x and z are the horizontal and vertical coordinates (L), respectively. Eq. (3) is

the form of the variably saturated flow equation which is solved in this paper. As discussed below, this mixed form of the variably saturated flow equation has numerical advantages as well as physical significance.

2.2. Numerical solution to the two-dimensional, variably saturated flow equation

A fully implicit, finite-difference approximation of the spatial terms in Eq. (3), using a Picard iteration scheme for the nonlinear terms can be written as

$$\begin{aligned}
 & \frac{\partial}{\partial x} \left\{ K(\theta) \frac{\partial \Psi}{\partial x} \right\} + \frac{\partial}{\partial z} \left\{ K(\theta) \frac{\partial \Psi}{\partial z} \right\} + \frac{\partial K(\theta)}{\partial z} \\
 & \approx \frac{1}{\Delta x} \left[\left(\frac{K_{ij}^{n+1,m} + K_{i+1j}^{n+1,m}}{2} \right) \left(\frac{\Psi_{i+1j}^{n+1,m+1} - \Psi_{ij}^{n+1,m+1}}{\Delta x} \right) \right. \\
 & \quad \left. - \left(\frac{K_{ij}^{n+1,m} + K_{i-1j}^{n+1,m}}{2} \right) \left(\frac{\Psi_{ij}^{n+1,m+1} - \Psi_{i-1j}^{n+1,m+1}}{\Delta x} \right) \right] \\
 & + \frac{1}{\Delta z} \left[\left(\frac{K_{ij}^{n+1,m} + K_{ij+1}^{n+1,m}}{2} \right) \left(\frac{\Psi_{ij+1}^{n+1,m+1} - \Psi_{ij}^{n+1,m+1}}{\Delta z} \right) \right. \\
 & \quad \left. - \left(\frac{K_{ij}^{n+1,m} + K_{ij-1}^{n+1,m}}{2} \right) \left(\frac{\Psi_{ij}^{n+1,m+1} - \Psi_{ij-1}^{n+1,m+1}}{\Delta z} \right) \right] \\
 & + \frac{1}{\Delta z} \left[\left(\frac{K_{ij}^{n+1,m} + K_{ij+1}^{n+1,m}}{2} \right) - \left(\frac{K_{ij}^{n+1,m} + K_{ij-1}^{n+1,m}}{2} \right) \right] \quad (4)
 \end{aligned}$$

where n denotes the n th discrete time level, t^n , when the solution is known, $\Delta t = t^{n+1} - t^n$ is the time step, and m is the Picard iteration level. K_{ij} is the value of hydraulic conductivity at node ij , and Ψ_{ij} is the pressure head at that node. $K(\theta)$ is a nonlinear function of θ ; it is linearized using a Picard iteration scheme. The current and previous Picard iteration levels are denoted as $m+1$ and m , respectively. It should be noted that the hydraulic conductivity is arithmetically averaged between nodes, rather than employing an alternative scheme using the geometric or harmonic mean, for example. Use of the arithmetic mean is justified by the finding of Kirkland et al. (1992) that solution of the closely related Richards' equation is relatively insensitive to the interblock-averaging scheme used for hydraulic conductivity. Kirkland et al. (1992) also found that use of a Crank–Nicholson scheme on the closely related mixed form of Richards' equation fails to reduce truncation error, and is, of course, subject to potential instabilities; consequently, the fully implicit formulation is used herein.

Temporal variations in storage owing to changes in pressure are approximated using a backward Euler, finite-difference expression for the first term of the left

side of Eq. (3):

$$\frac{S_s \theta}{\eta} \frac{\partial \Psi}{\partial t} \approx \frac{S_s}{\eta} \theta_{ij}^{n+1,m} \left[\frac{\Psi_{ij}^{n+1,m+1} - \Psi_{ij}^n}{\Delta t} \right] \quad (5)$$

where the superscripts n and m indicate the time iteration and Picard iteration levels, respectively; and Δt is the time step, which, in general, is set to maintain acceptably small temporal variations in Ψ .

A backward Euler approximation, coupled with a Picard iteration scheme, is used to discretize the second term of the left side of Eq. (3), containing the time derivative of water content:

$$\frac{\partial \theta}{\partial t} \approx \left[\frac{\theta_{ij}^{n+1,m+1} - \theta_{ij}^n}{\Delta t} \right] \quad (6)$$

After Celia et al. (1990), $\theta_{ij}^{n+1,m+1}$ is expanded using a first-order, truncated Taylor series, in terms of the pressure-head perturbation arising from Picard iteration, about the expansion point $(\theta_{ij}^{n+1,m}, \Psi_{ij}^{n+1,m})$, as

$$\theta_{ij}^{n+1,m+1} \approx \theta_{ij}^{n+1,m} + \left. \frac{d\theta}{d\Psi} \right|_{ij}^{n+1,m} [\Psi_{ij}^{n+1,m+1} - \Psi_{ij}^{n+1,m}] \quad (7)$$

The specific water capacity of a soil (L^{-1}) is defined as

$$C(\Psi) = \frac{d\theta}{d\Psi} \quad (8)$$

Using Eqs. (6)–(8), the (partial) time derivative of water content is approximated:

$$\frac{\partial \theta}{\partial t} \approx \left[\frac{\theta_{ij}^{n+1,m} - \theta_{ij}^n}{\Delta t} \right] + C_{ij}^{n+1,m} \left[\frac{\Psi_{ij}^{n+1,m+1} - \Psi_{ij}^{n+1,m}}{\Delta t} \right] \quad (9)$$

The first term on the right side of Eq. (9) is an explicit estimate for the (partial) time derivative of water content, based on the m th Picard level estimates of pressure head. In the second term of the right side of Eq. (9), the numerator of the bracketed fraction is an estimate of the error in the pressure head at node ij between two successive Picard iterations. Its value diminishes as the Picard iteration process converges. As a result, as the Picard process proceeds, the contribution of the specific water capacity, $C(\Psi)$, is diminished. This behavior, coupled with the fact that the specific water capacity is used only in the derivative term of the Taylor series expansion of the temporal derivative of the moisture content (see Eq. (7)), distinguishes this numerical solution (espoused by Celia et al. (1990)) of the (mixed form of the) variably saturated equation from that of the pressure-based form.

The finite-difference expressions for the spatial and temporal derivatives, Eqs. (4), (5) and (9), are rearranged by collecting all the unknowns on the left side and all the knowns on the right, in agreement with Eq. (3). Using the above implicit finite-difference approximation, the pressure heads at the $(n+1)$ th time level and

$(m + 1)$ th Picard level are obtained from solution of the following system of simultaneous linear algebraic equations:

$$\begin{aligned} a\Psi_{ij-1}^{n+1,m+1} + b\Psi_{i-1j}^{n+1,m+1} + c\Psi_{ij}^{n+1,m+1} + d\Psi_{i+1j}^{n+1,m+1} + e\Psi_{ij+1}^{n+1,m+1} \\ = -f_1\Psi_{ij}^{n+1,m} - f_2\Psi_{ij}^n + g + h \end{aligned} \quad (10)$$

where coefficients $a, b, c, d, e, f_1, f_2, g$ and h are defined as

$$\begin{aligned} a &= \left(\frac{K_{ij}^{n+1,m} + K_{ij-1}^{n+1,m}}{2\Delta z^2} \right), & b &= \left(\frac{K_{ij}^{n+1,m} + K_{i-1j}^{n+1,m}}{2\Delta x^2} \right) \\ d &= \left(\frac{K_{ij}^{n+1,m} + K_{i+1j}^{n+1,m}}{2\Delta x^2} \right), & e &= \left(\frac{K_{ij}^{n+1,m} + K_{ij+1}^{n+1,m}}{2\Delta z^2} \right) \\ f_1 &= \frac{C_{ij}^{n+1,m}}{\Delta t}, & f_2 &= \frac{S_s\theta_{ij}^{n+1,m}}{\eta\Delta t} \\ g &= -\left(\frac{K_{ij+1}^{n+1,m} - K_{ij-1}^{n+1,m}}{2\Delta z} \right), & h &= \left[\frac{\theta^{n+1,m} - \theta^n}{\Delta t} \right] \end{aligned}$$

and

$$c = -[a + b + d + e + f_1 + f_2] \quad (11)$$

Eq. (10) applies to all interior nodes; at boundary nodes this equation is modified to reflect the appropriate boundary conditions. The resulting set of consistent linear algebraic equations, for the unknown pressure-head values, is written in a matrix notation:

$$\mathbf{A}\hat{\Psi} = \hat{\mathbf{b}} \quad (12)$$

where $\hat{\Psi}$ is the vector of unknown pressure heads, $\Psi_{ij}^{n+1,m+1}$, $\hat{\mathbf{b}}$ is the forcing vector, and Ψ_{ij}^n is the pressure head at the previous time step. \mathbf{A} is a square matrix consisting of the coefficients of the finite-difference Eq. (10). \mathbf{A} is banded for problems discretized into rectangular grids.

2.3. Numerical solution of the linearized system of equations

Eq. (12) is solved using the conjugate-gradient method, an iterative procedure which solves matrix problems by minimizing residuals. A complete description of the conjugate-gradient method has been given by Golub and Van Loan (1983, p. 362). This method has several features which make it the logical choice for solving transient problems with a banded matrix. The conjugate-gradient method never requires the complete matrix \mathbf{A} . It needs only the vector product $\mathbf{A}\hat{\mathbf{d}}^k$, where $\hat{\mathbf{d}}^k$ is the directional vector at (conjugate-gradient) iteration level k . The nonzero bands in \mathbf{A} are stored as one-dimensional vectors and a specialized matrix-multiplier routine is used to compute the vector product $\mathbf{A}\hat{\mathbf{d}}^k$. To compute the initial directional vector $\hat{\mathbf{d}}^k$, the conjugate-gradient method requires an initial guess for $\hat{\Psi}^0$, containing the

pressures at all nodes. These initial estimates are iteratively updated as the process converges toward the solution. As the time steps used in the transient simulations are relatively small, changes in the pressures during each time step are, in general, quite gradual. Consequently, the solution for a given time step is usually an excellent guess for the next, so the solution converges quickly within a few iterations, minimizing computational effort. Convergence is further improved by preconditioning A ; herein, the Jacobi preconditioner is used (Golub and Van Loan, 1983, p. 374). Other methods, such as incomplete Cholesky preconditioning, can also be used to accelerate convergence.

2.4. Soil properties

Van Genuchten's (1980) closed-form equation for the soil water retention curve and Mualem's (1976) unsaturated hydraulic conductivity function are used to describe the soil properties. The relationship between water content and pressure head (under tension) is given by (Van Genuchten, 1980)

$$\Theta = \left\{ \frac{1}{1 + (\alpha_v |\Psi|)^{n_v}} \right\}^{m_v} \quad (13)$$

where α_v , n_v , and $m_v = 1 - (1/n_v)$ are the Van Genuchten parameters, whose values depend upon the soil properties. The parameter α_v is a measure of the first moment of the pore size density function (L^{-1}) (as α_v increases, so does the first moment), and n_v is an inverse measure of the second moment of the pore size density function (Wise, 1991) (as n_v increases, the pore size density function becomes narrower). Θ is the effective saturation, given by the relationship

$$\Theta = \frac{\theta - \theta_r}{\theta_s - \theta_r} \quad (14)$$

where θ_s is the saturated water content (often approximated by the porosity η) and θ_r is the residual water content of the soil. Of course, for nonnegative Ψ , $\Theta = 1$, that is, the medium is saturated.

Based on Mualem's (1976) model, the relationship between water content and hydraulic conductivity is given by (Van Genuchten, 1980)

$$K(\Theta) = K_s \{1 - \{1 - \Theta^{(1/m_v)}\}^{m_v}\}^2 \Theta^{(1/2)} \quad (15)$$

where K_s is the saturated hydraulic conductivity. It should be noted that the relative permeability, $K(\Theta)/K_s$, does not depend upon the value of α_v .

2.5. Boundary conditions

Dirichlet, Neumann, and seepage-face boundaries are considered. For each, Eq. (10) is modified as necessary.

Dirichlet boundaries

Dirichlet nodes, where the pressure heads are known, are described by:

$$\Psi_{ij} = \dagger\Psi_{ij} \quad (16)$$

where $\dagger\Psi_{ij}$ are the known pressure heads at the nodes ij . For Dirichlet nodes, the matrix coefficients a , b , d , e , and g in the finite-difference Eq. (10) are zero, and c equals unity. Furthermore, the known pressure heads $\dagger\Psi_{ij}$ are identically the corresponding ij terms in the forcing vector \hat{b} .

Neumann boundaries

Values of normal fluxes, q_n , are specified at Neumann (or flux) boundary nodes. Using Darcy's law in (forward) finite-difference form, the horizontal flux at a (right) boundary node is written

$$q_x \approx - \left[\frac{K_{i+1j} + K_{ij}}{2} \right] \left[\frac{\Psi_{i+1j} - \Psi_{ij}}{\Delta x} \right] \quad (17)$$

where q_x is the specified Darcy flux in the x direction at the node ij . At a (right) no-flow boundary,

$$\Psi_{i+1j} = \Psi_{ij} \quad (18)$$

Using Eqs. (18) and (10), the finite-difference equation for a (right) no-flow boundary is written

$$\begin{aligned} a\Psi_{ij-1}^{n+1,m+1} + b\Psi_{i-1j}^{n+1,m+1} + (c+d)\Psi_{ij}^{n+1,m+1} + e\Psi_{ij+1}^{n+1,m+1} \\ = -f_1\Psi_{ij}^{n+1,m} - f_2\Psi_{ij}^n + g + h \end{aligned} \quad (19)$$

For Neumann nodes in the vertical direction, Darcy's law also includes the gravity term. For vertical flow, Darcy's law is expressed in finite-difference form (for a top node) by

$$q_z \approx - \left[\frac{K_{ij+1} + K_{ij}}{2} \right] \left[\frac{\Psi_{ij+1} - \Psi_{ij}}{\Delta z} - 1 \right] \quad (20)$$

Similar to the treatment of the horizontal flux boundary, Eq. (20) is used to modify Eq. (10) for vertical flux boundary nodes.

Seepage-face boundaries

A seepage face is an external boundary of the saturated zone where water leaves the soil and Ψ is uniformly zero. When the length of the seepage face is known a priori, all the nodes along the seepage face are treated as Dirichlet nodes with the prescribed pressure head, $\Psi = 0$. Nodes above the seepage face are specified as no-flow nodes. During simulation of both steady-state and transient variably saturated flow, the length of the seepage face is unknown until the problem is solved. However, the boundary conditions cannot be completely specified to solve the problem unless the length of the seepage face is known. Hence, the seepage face must be determined using an iterative process. The location of the seepage face is guessed during the first

Table 2
Summary of simulation parameters for examples 1–4

Example	Reference for data	K_s (m day ⁻¹)	θ_s	θ_r	α_v (m ⁻¹)	n_v	A	B	C	D	Δx (m)	Δz (m)	Δt_{\min} (s)	Δt_{\max} (s)
1	Hall (1955)	397	0.43	0	9.0	4.0	–	–	–	–	0.036 (Δr)	0.024	–	–
2	Haverkamp et al. (1977)	8.16	0.287	0.075	–	–	1.61×10^6	3.96	1.18×10^6	4.74	0.01	0.01	3.6	36
3	Vaucelin et al. (1979)	8.40	0.30	0.01	3.3	4.1	–	–	–	–	0.10	0.05	8.6	346
4	Vaucelin et al. (1975)	9.60	0.30	0	–	–	4.00×10^4	2.90	3.60×10^5	4.50	0.10	0.05	3.6	360

iteration, and this intermediate problem (Eq. (3), subject to the various imposed initial and boundary conditions) is solved. If the location of the seepage face is correct, then the solution gives a net outward flux in all the nodes along the seepage face, where Ψ is zero. Values for Ψ at all the boundary nodes above the seepage face where flux is set to zero are negative. If the height of the seepage face is overestimated, some of the boundary nodes where Ψ is assumed to be zero have nonzero fluxes directed inward. On the other hand, if the seepage-face height is underestimated, boundary nodes above the seepage face, where flux is set to zero, have positive values for Ψ . In either case, the fundamental physics of the variably saturated flow problem are violated for incorrect specification of the seepage-face height. Using these principles, Neuman's (1973) iterative-search procedure, as modified by Cooley (1983), is used to determine the seepage face length.

2.6. Iteration levels within the algorithm

There are three nested iterative procedures executed during each time step. Innermost among these is the conjugate gradient method to solve the system of equations subject to the Picard linearization scheme, which forms the intermediate iteration level. These iterations take place within the iterative search for the seepage face.

3. Algorithm reproduction of published experimental results

Based upon the above narrative, a two-dimensional, finite-difference, variably saturated algorithm has been developed to simulate two-dimensional water movement through variably saturated porous media. Below, the performance of the algorithm is compared with four published, illustrative sets of experimental data, each representing a different physical scenario. The parameters used in these four numerical simulations are presented in Table 2.

3.1. Example 1: steady-state radial flow to a well

This example involves simulation of the sand-filled, wedge-shaped tank, phreatic-surface data collected by Hall (1955). As this problem involves radial flow, the algorithm must be accordingly modified. The governing equation for variably saturated flow, Eq. (2), is written in radial coordinates as

$$\frac{\theta}{\eta} S_s \frac{\partial \Psi}{\partial t} + \frac{\partial \theta}{\partial t} = \frac{1}{r} \frac{\partial}{\partial r} \left\{ r K(\theta) \frac{\partial \Psi}{\partial r} \right\} + \frac{\partial}{\partial z} \left\{ K(\theta) \frac{\partial \Psi}{\partial z} \right\} + \frac{\partial K(\theta)}{\partial z} \quad (21)$$

where r is the radial distance (L) from the origin. For steady-state conditions, the time derivatives on the left side of Eq. (21) are identically zero:

$$0 = \frac{1}{r} \frac{\partial}{\partial r} \left\{ r K(\theta) \frac{\partial \Psi}{\partial r} \right\} + \frac{\partial}{\partial z} \left\{ K(\theta) \frac{\partial \Psi}{\partial z} \right\} + \frac{\partial K(\theta)}{\partial z} \quad (22)$$

This problem is schematically illustrated in Fig. 1. The boundary conditions are

$$\begin{array}{lll}
 \Psi = 1.22 \text{ m} - z & r = 1.95 \text{ m} & 0 \leq z \leq 1.22 \text{ m} \\
 q_z = 0 & 0.122 \leq r \leq 1.95 \text{ m} & z = 0 \text{ and } z = 1.22 \text{ m} \\
 \Psi = 0.305 \text{ m} - z & r = 0.122 \text{ m} & 0 \leq z \leq 0.305 \text{ m} \\
 \Psi = 0 & r = 0.122 \text{ m} & 0.305 \text{ m} < z \leq H_s \\
 q_x = 0 & r = 0.122 \text{ m} & H_s < z \leq 1.22 \text{ m}
 \end{array}$$

where 0.122 m is the radius of the well, 1.22 m is the height of the apparatus, 1.95 m is the length of the apparatus, 0.305 m is the height of water inside the well, and H_s is the height of the seepage face (L). The saturated hydraulic conductivity of the sand used is 397 m day^{-1} ; however, the positions of the phreatic surface and the seepage face are not dependent on the value of the saturated hydraulic conductivity for steady flow. The residual saturation is taken as $\theta_r = 0$. Van Genuchten soil parameters for Hall’s sand are fitted to be $\alpha_v = 9.0 \text{ m}^{-1}$ and $n_v = 4.0$, from speculations on the capillary properties of this medium made by Taylor and Luthin (1969). In this problem, it is assumed that the values of the relative hydraulic conductivity are exactly equal to the local effective saturation, θ/η , following Cooley (1983). This approximation is valid owing to the narrow distribution ($n_v = 4.0$) of large pores ($\alpha_v = 9.0 \text{ m}^{-1}$) which drain very rapidly under suction, hence, rapidly diminishing permeability at sub-atmospheric pressures. Furthermore, Clement et al. (1994) demonstrated through

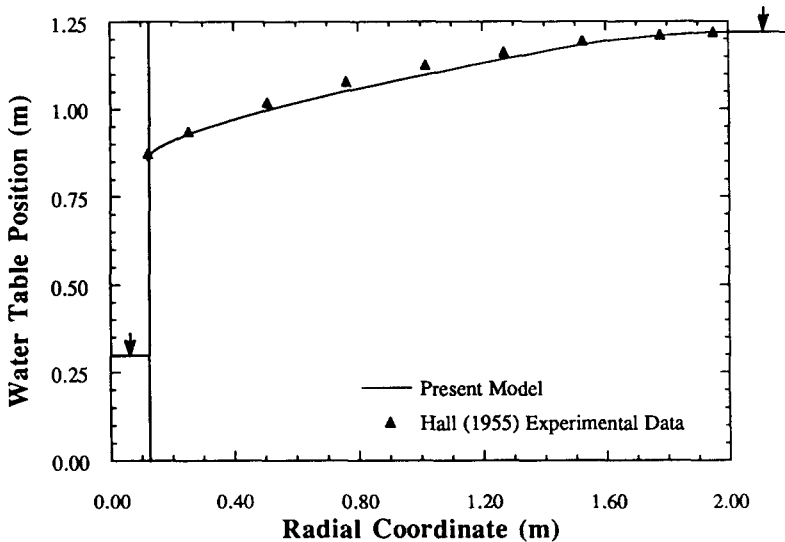


Fig. 1. Simulation of steady-state, water-table data for a sand-filled, wedge-shaped (radial-flow) tank collected by Hall (1955).

sensitivity analyses that the hydraulic behavior in such steady-state radial-flow problems is relatively insensitive to capillary properties of the porous medium used.

Numerical results predicted by the algorithm are compared with Hall's (1955) data in Fig. 1, which illustrates that there is good agreement between the water-table position predicted by the present model and that observed by Hall.

3.2. Example 2: transient infiltration in a vertical soil column

This example, modeling data from Haverkamp et al. (1977), is selected to verify the pressure-head and water-content predictions of the present algorithm during transient flow with an infiltration boundary. The problem concerns one-dimensional infiltration into a sand column. A constant pressure head of $\Psi = -0.615$ m is maintained at the lower end of the column and a constant flux of 3.29 m day⁻¹ is imposed at the soil surface. This problem was studied in the laboratory using a Plexiglas column; the details of the experimental techniques have been presented by Vachaud and Thony (1971). The observed water content profiles during an infiltration experiment, of 0.8 h duration, into a 0.70 m long column have been reported by Haverkamp et al. (1977). In the present study, the flow region is modeled as a rectangular column, 0.70 m tall and 0.05 m wide. No-flow boundary conditions are specified along both sides of the column. The porosity and residual water content of the soil are $\eta = \theta_s = 0.287$ and $\theta_r = 0.075$, respectively. The saturated hydraulic conductivity of the soil, K_s , is 8.16 m day⁻¹. Haverkamp et al. (1977) fitted an analytical expression for the capillary pressure function to experimental data:

$$\theta = \frac{A(\theta_s - \theta_r)}{A + (100|\Psi|)^B} + \theta_r \quad (23)$$

where $\eta = \theta_s$ is the porosity, θ_r is residual water content, Ψ is the pressure head in meters, and the values of A and B are 1.61×10^6 and 3.96, respectively.

Their analytical expression for the relative hydraulic conductivity is given by

$$K_r(\Psi) = \frac{C}{C + (100|\Psi|)^D} \quad (24)$$

where K_r is the relative hydraulic conductivity, and the values of C and D are 1.18×10^6 and 4.74, respectively. The algorithm is easily modified to handle these expressions for the soil water retention curve and the relative permeability function.

For the numerical simulation, the initial pressure head is set to -0.615 m throughout the column. The soil is subjected to a constant infiltration of 3.29 m day⁻¹ for 0.8 h. Node spacings in the x and z directions are $\Delta x = 0.01$ m and $\Delta z = 0.01$ m, respectively. Transient pressure-head distributions in the column are simulated with time steps, Δt , ranging from 3.6 to 36.0 s.

Simulated water-content distributions, at 0.1 h time intervals, are compared with experimentally observed water content values in Fig. 2, in which it is seen that there is good agreement between the experimental data and the water content profiles predicted by the present algorithm.

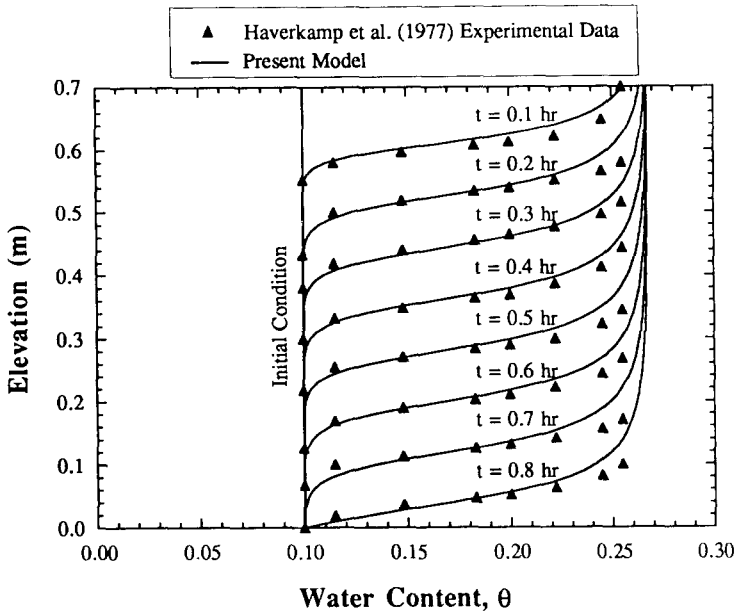


Fig. 2. Simulation of transient infiltration data for a sand-filled column collected by Haverkamp (1977).

3.3. Example 3: transient, two-dimensional, variably saturated water-table recharge

This example is selected to verify the performance of the algorithm for two-dimensional, transient, variably saturated flow conditions. The experiment has been presented in detail by Vauclin et al. (1979). The flow domain consisted of a rectangular soil slab, $6.00 \text{ m} \times 2.00 \text{ m}$, with an initial horizontal water table located at a height of 0.65 m . At the soil surface, a constant flux of $q = 3.55 \text{ m day}^{-1}$ was applied over a width of 1.00 m in the center. The remaining soil surface was covered to prevent evaporation losses. Because of the symmetry, only one side (here the right side) of the flow domain needs to be modeled. As illustrated in Fig. 3, the modeled portion of the flow domain is $3.00 \text{ m} \times 2.00 \text{ m}$, with no-flow boundaries on the bottom and on the left side (accounting for the symmetry). At the soil surface, the constant flux of 3.55 m day^{-1} is applied over the left 0.50 m of the top of the modeled domain. The remaining soil surface at the top is a no-flow boundary. The water level at the right face of the block is maintained at 0.65 m . As this problem has a steady-state solution (both experimental (Vauclin et al., 1979) and numerical) without development of a seepage face, a no-flow boundary is used above the water table on the right side of the domain.

From Vauclin et al. (1979), the soil properties used in the model are a saturated hydraulic conductivity of 8.40 m day^{-1} , a porosity of $\eta = \theta_s = 0.30$, and a residual saturation of $\theta_r = 0.01$. The Van Genuchten (1980) model is fitted to the water retention and the relative hydraulic conductivity data given by Vauclin et al. (1979); the estimated values for the soil properties are $\alpha_v = 3.3 \text{ m}^{-1}$ and $n_v = 4.1$.

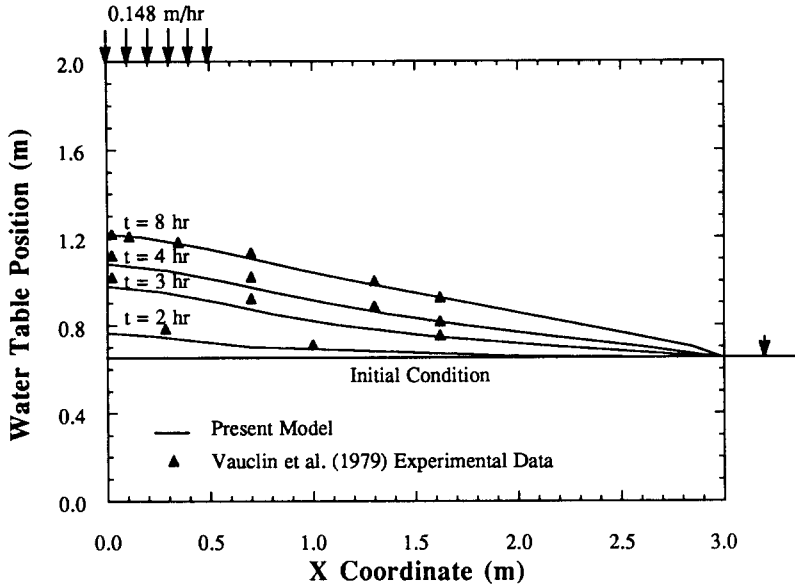


Fig. 3. Simulation of transient, water-table mounding data collected by Vauclin et al. (1979).

Specific storage may be neglected for this problem because changes in storage are facilitated by the filling of pores, which overshadows the effects of compressibility for the vertical extent of this flow domain; hence, the specific storage coefficient is set to zero.

The nodal spacing in the x and z directions are $\Delta x = 0.10$ m and $\Delta z = 0.05$ m, respectively. The soil system is assumed to be initially at hydrostatic equilibrium with respect to the water table throughout the flow domain. Transient simulations are performed using time steps varying from $\Delta t = 8.64$ s to $\Delta t = 346$ s.

Transient positions of the water table are compared with the experimental results presented by Vauclin et al. (1979) in Fig. 3, which illustrates that there is excellent agreement between the transient water-table positions predicted by the algorithm and those observed.

3.4. Example 4: transient, two-dimensional, unconfined drainage

This example is chosen to verify the performance of the algorithm in modeling transient, unconfined drainage problems with seepage-face boundaries. Vauclin et al. (1975) presented experimental data for the transient locations of the seepage face and water table in a two-dimensional drainage problem. A 6.00 m \times 2.00 m saturated porous medium was allowed to drain after a sudden drop in the external water table. Water contents and pressure heads were measured during the entire transient drainage phase until the steady-state conditions were reached. Details of this experiment have been discussed by Vauclin et al. (1975).

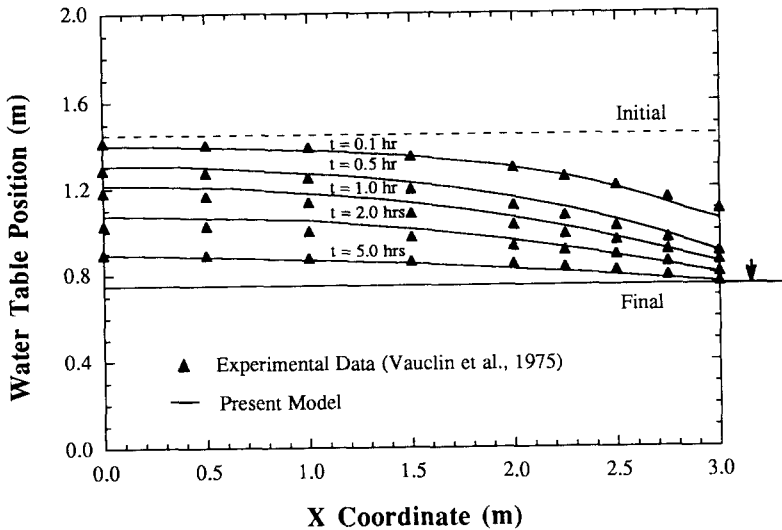


Fig. 4. Simulation of transient drainage data collected by Vauclin et al. (1975).

Owing to the symmetry of this problem, for numerical purposes, it is sufficient to model only one side of the flow domain. Illustrated in Fig. 4 is the right-hand side of the modeled flow domain. As seen from the figure, the $3.00 \text{ m} \times 2.00 \text{ m}$ flow model has no-flow boundaries on the bottom, top, and on the left side (accounting for the symmetry). Before drainage, the water table is maintained at the height of 1.45 m; the system is assumed to be in static equilibrium. At the time $t = 0$, the external water table is dropped instantaneously to the height of 0.75 m, and is maintained there subsequently. The temporal location of the seepage face is unknown until the problem is solved at a given time. Hence, on the right side, the seepage-face boundary is transiently determined between the height of 0.75 m and 1.45 m. Below the external water-table level of 0.75 m, a constant head boundary of $h = \Psi + z = 0.75 \text{ m}$ is applied.

The water retention of the soil is represented by Eq. (23), using values of $A = 4.00 \times 10^5$, $B = 2.90$, $\eta = \theta_s = 0.3$ and $\theta_r = 0$ (Vauclin et al., 1975). Similarly, the relative hydraulic conductivity function is described by Eq. (24), using values of $C = 3.60 \times 10^5$ and $D = 4.50$, and the saturated hydraulic conductivity is $K_s = 9.6 \text{ mday}^{-1}$ (Vauclin et al., 1975). As the pressure drop in the external water table is not very large (0.70 m), the specific storage effects are minimal; a small value of specific storage coefficient, $S_s = 10^{-6} \text{ m}^{-1}$ (almost corresponding to the compressibility of water), is used in this simulation. The nodal spacings in the x and z directions are $\Delta x = 0.10 \text{ m}$ and $\Delta z = 0.05 \text{ m}$, respectively. The transient simulation is continued until steady state is approached.

Numerically simulated water-table positions are compared with Vauclin et al.'s (1975) experimental results in Fig. 4, in which it is seen that the numerical model is able to reproduce closely the experimental results.

4. Discussion

A general, two-dimensional, finite-difference algorithm is developed above for modeling variably saturated flow through porous media. The algorithm performs well over a broad range of problems, as demonstrated by its performance against published experimental data. The generality of the algorithm arises from its direct statement of the governing physics of variably saturated flow. Solutions obtained are mass conserving within the unsaturated zone, owing to the form of and solution procedure for the governing equation. The algorithm is demonstrated to work well for infiltration fronts, and steady-state and transient water tables, as well as steady-state and transient seepage faces, in both Cartesian and radial coordinate systems.

The algorithm is based upon central differences in space, implicit formulation in time, and a modified Picard iteration to handle the nonlinearity of the governing equation. The difference equations, forming a simultaneous set of linear algebraic equations, are solved using the preconditioned conjugate gradient method. The algorithm is relatively easy to code and is found to be computationally efficient.

The success of the algorithm in simulating a variety of problems lends confidence to its application for many variably saturated flow problems. This belief is supported by the comprehensive statement of the governing equation, as well as the mass-conserving nature of the solution method. The algorithm has been used to solve a variety of steady-state and transient seepage-face problems. Results from these studies have been given by Clement et al. (1994) and Wise et al. (1994), respectively.

5. Acknowledgments

This work was supported, in part, by the US Environmental Protection Agency (Contract CR-818717-01-0) through the Environmental Research Laboratory in Athens, Georgia. However, it has not been through the agency's required peer and administrative review. Therefore, it does not necessarily reflect the views of the agency, and no official endorsement should be inferred.

6. References

- Allen, M.B. and Murphy, C.L., 1986. A finite element collocation method for variably saturated flow in two space dimensions. *Water Resour. Res.*, 22(11): 1537–1542.
- Brandt, A., Bresler, E., Diner, N., Ben-Asher, L., Heller, J. and Goldman, D., 1971. Infiltration from a trickle source: 1. Mathematical models. *Soil Sci. Soc. Am. Proc.*, 35: 675–689.
- Brutsaert, W.F., 1971. A functional iteration technique for solving the Richards' equation applied to two-dimensional infiltration problems. *Water Resour. Res.*, 7(6): 1538–1596.
- Celia, M.A., Bouloutas, E.T. and Zarba, R.L., 1990. A general mass-conservative numerical solution of the unsaturated flow equation. *Water Resour. Res.*, 26: 1483–1496.
- Clement, T.P., Wise, W.R., Molz, F.J. and Wen, M., 1994. A comprehensive study of the modeling of steady-state seepage faces. *Water Resour. Res.*, submitted.
- Cooley, R.L., 1971. A finite difference method for unsteady flow in variably saturated porous media: application to a single pumping well. *Water Resour. Res.*, 7: 1607–1625.

- Cooley, R.L., 1983. Some new procedures for numerical solution of variably saturated flow problems. *Water Resour. Res.*, 19: 1271–1285.
- Dane, J.H. and Mathis, F.H., 1981. An adaptive finite difference scheme for the one-dimensional water flow equation. *Soil Sci. Soc. Am. J.*, 45: 1048–1054.
- Day, P.R. and Luthin, J.N., 1956. A numerical solution of the differential equation of flow for a vertical drainage problem. *Soil Sci. Soc. Am. Proc.*, 20: 443–446.
- Dullien, F.A.L., 1979. *Porous Media Fluid Transport and Pore Structure*. Academic Press, San Diego, CA, 396 pp.
- Freeze, R.A., 1969. The mechanism of natural groundwater recharge and discharge 1. One-dimensional, vertical, unsteady, unsaturated flow above a recharging and discharging groundwater flow system. *Water Resour. Res.*, 5: 153–171.
- Freeze, R.A., 1971a. Three dimensional transient, saturated–unsaturated flow in a groundwater basin. *Water Resour. Res.*, 7: 347–366.
- Freeze, R.A., 1971b. Influence of the unsaturated flow domain on seepage through earth dams. *Water Resour. Res.*, 7: 929–941.
- Golub, G.H. and van Loan, C.F., 1983. *Matrix Computations*. Johns Hopkins University Press, Baltimore, MD, 476 pp.
- Hall, H.P., 1955. An investigation of steady state flow toward a gravity well. *Houille Blanche*, 10: 8–35.
- Haverkamp, R. and Vauclin, M., 1981. A comparative study of three forms of the Richards' equation used for predicting one-dimensional infiltration in unsaturated soil. *Soil Sci. Soc. Am. J.*, 45: 13–20.
- Haverkamp, R., Vauclin, M., Touma, J., Wierenga, P.J. and Vachaud, G., 1977. Comparison of numerical simulation models for one-dimensional infiltration. *Soil Sci. Soc. Am. J.*, 41: 285–294.
- Healy, R.W., 1990. Simulation of solute transport in variably saturated porous media with supplemental information on modifications to the US Geological Survey's computer program VS2D. *US Geol. Surv. Water-Resour. Invest. Rep.*, 90-4025.
- Huyakorn, P.S., Thomas, S.D. and Thompson, B.M., 1984. Techniques for making finite elements competitive in modeling flow in variably saturated media. *Water Resour. Res.*, 20: 1099–1115.
- Huyakorn, P.S., Springer, E.P., Guvanasen, V. and Wadsworth, T.D., 1986. A three dimensional finite-element model for simulating water flow in variably saturated porous media. *Water Resour. Res.*, 22: 1790–1808.
- Kirkland, M.R., 1991. Algorithms for solving Richards' equation for variably saturated soils. Ph.D. Thesis, Department of Mechanical Engineering, New Mexico State University, Las Cruces.
- Kirkland, M.R., Hills, R.G. and Wierenga, P.J., 1992. Algorithms for solving Richards' equation for variably saturated soils. *Water Resour. Res.*, 28: 2049–2058.
- Mualem, Y., 1976. A new model for predicting hydraulic conductivity of unsaturated porous media. *Water Resour. Res.*, 12: 513–522.
- Narasimhan, T.N. and Witherspoon, P.A., 1976. An integrated finite difference method for analyzing fluid flow in porous media. *Water Resour. Res.*, 12(1): 57–64.
- Narasimhan, T.N., Witherspoon, P.A. and Edwards, A.L., 1978. Numerical model for saturated–unsaturated flow in deformable porous media, 2. The algorithm. *Water Resour. Res.*, 14: 255–261.
- Neuman, S.P., 1973. Saturated–unsaturated seepage by finite elements. *J. Hydraul. Div. ASCE*, 99(HY12): 2233–2250.
- Panday, S., Huyakorn, P.S., Therrien, R. and Nichols, R.L., 1993. Improved three-dimensional finite-element techniques for field simulation of variably saturated flow and transport. *J. Contaminant Hydrol.*, 12: 3–33.
- Pinder, G.F. and Gray, W.G., 1977. *Finite Element Simulation in Surface and Subsurface Hydrology*. Academic Press, New York.
- Rubin, J., 1968. Theoretical analysis of two-dimensional, transient flow of water in unsaturated and partly saturated soils. *Soil Sci. Soc. Am. Proc.*, 32: 607–615.
- Taylor, G.S. and Luthin, J.N., 1969. Computer methods for transient analysis of water table aquifers. *Water Resour. Res.*, 5(1): 144–152.
- Vachaud, G. and Thony, J.L., 1971. Hysteresis during infiltration and redistribution in a soil column at different initial water contents. *Water Resour. Res.*, 7(1): 111–127.

- Van Genuchten, M.Th., 1980. A closed-form equation for predicting the hydraulic conductivity of unsaturated soils. *Soil Sci. Soc. Am. J.*, 44: 892–898.
- Vauclin, M., Khanji, D. and Vachaud, G., 1979. Experimental and numerical study of a transient, two-dimensional unsaturated–saturated water table recharge problem. *Water Resour. Res.*, 15(5): 1089–1101.
- Vauclin, M., Vachaud, G. and Khanji, J., 1975. Two dimensional numerical analysis of transient water transfer in saturated-unsaturated soils. In: G.C. Vansteenkiste (Editor), *Modeling and Simulation of Water Resources Systems*, North-holland, Amsterdam, pp. 299–323.
- Whisler, F.D. and Watson, K.K., 1968. One-dimensional gravity drainage of uniform columns of porous materials. *J. Hydrol.*, 6: 277–296.
- Wise, W. R., 1991. Discussion of “On the relation between saturated conductivity and capillary retention characteristics”, by S. Mishra and J.C. Parker, September–October 1990 issue, v. 28, no. 5, pp. 775–777. *Ground Water*, 29(2): 272–273.
- Wise, W.R., Clement, T.P. and Molz, F.J., 1994. Variably saturated modeling of transient drainage: sensitivity to soil properties. *J. Hydrol.*, 161: 91–108.
- Yeh, G.T., 1992. *Users’ Manual: A Finite Element Model of WATER Flow through Saturated–Unsaturated Porous Media*. Department of Civil Engineering, The Pennsylvania State University.
- Yeh, G.T. and Ward, D.S., 1981. *FEMWATER: a finite-element model of water flow through saturated–unsaturated porous media*. Rep. ORNL-5601, Oak Ridge National Laboratory, Oak Ridge, TN.